



Published in final edited form as:

Interdiscip Sci. 2009 December ; 1(4): 254–262. doi:10.1007/s12539-009-0052-7.

Computational Modeling Study of Human Nicotinic Acetylcholine Receptor for Developing New Drugs in the Treatment of Alcoholism

Zeng-Jian Hu^{1,*}, Li Bai², Yousef Tizabi³, and William Southerland¹

¹Department of Biochemistry and Molecular Biology, Howard University College of Medicine, Washington, DC 20059, USA

²National Institute of Neurological Disorders and Stroke, Maryland 20892, USA

³Department of Pharmacology, Howard University College of Medicine, Washington, D. C. 20059, USA

Abstract

Alcohol abuse and alcoholism are serious and costly problem in USA. Thus, the development of anti-alcoholism agents could be very significant. The understanding of the neurochemical basis underlying the addictive properties of drugs of abuse is imperative for the development of new pharmacological means to reverse the addictive state, prevent relapse or to reduce the intake of addictive compounds. The nicotinic acetylcholine receptors (nAChRs) are important therapeutic targets for various diseases. Recent studies have revealed that the $\alpha 3\beta 2$, $\alpha 3\beta 3$, and $\alpha 6$ subunits of nAChR protein family might be pharmacological targets for developing new drugs in the treatment of alcoholism. We have performed computational homology modeling of the $\alpha 3\beta 2$, $\alpha 3\beta 3$, and $\alpha 6$ subunits of human nAChRs based upon the recently determined crystal structure of the extracellular domain (ECD) of the mouse nAChR $\alpha 1$ subunit complexed with α -bungarotoxin at 1.94 Å resolution. For comparison, we also built the ECD models of $\alpha 4\beta 2$, and $\alpha 7$ subunits of human nAChRs which are neurochemical targets for cessation of smoking. The three-dimensional (3D) models of the ECD of the monomer, and pentamer of these human nAChR were constructed. The docking of the agonist in the ligand-binding pocket of the human nAChR dimers was also performed. Since the nAChR ligand-binding site is a useful target for mutagenesis studies and the rational design of drugs against various diseases, these models provide useful information for future investigation.

Keywords

homology modeling; nicotinic acetylcholine receptor; molecular modeling; docking; ligand-binding interface; alcoholism

1 Introduction

Alcohol abuse and alcoholism are among the most serious and costly problems of Western society. In the United States, about 10% of the population abuse alcohol. The economic cost is more than \$185 billion every year (Gao *et al.*, 2003). Thus, the development of safe and effective anti-alcoholism agents is highly desirable. The understanding of the neurochemical basis underlying the addictive properties of alcohol abuse is imperative for the development

*Corresponding author. huzengjian@yahoo.com.

of new pharmacological means to reverse the addictive state, prevent relapse or to reduce the intake of addictive compounds. During the last few years new pharmacological strategies, most notably naltrexone and acamprosate (Spanagel and Kiefer, 2008), have been introduced for reducing alcohol consumption and preventing relapse in alcoholic patients.

Accumulating evidence from electrophysiological, pharmacological and neurochemical studies suggest that ethanol may interact with the nAChRs. It has been shown that the ethanol-induced stimulation of the mesolimbic dopamine system and of locomotor activity as well as ethanol intake and preference in rodents may involve central nAChRs. Additionally, data has been presented that nAChRs located in the ventral tegmental area may be of particular importance for these effects of ethanol (Larsson and Engel, 2004).

Recently studies aimed at defining the nAChRs sub-units involved in mediating ethanol-induced locomotor stimulation and accumbal dopamine overflow as well as ethanol intake have revealed that the $\alpha 3\beta 2$, $\alpha 3\beta 3$, and/or $\alpha 6$ subtypes of nAChR protein family could constitute neurochemical targets for developing new drugs in the treatment of alcoholism (Jerlhag *et al.*, 2008; Jerlhag *et al.*, 2006; Narahashi *et al.*, 1999), which arouses our interest to design small molecule agonists of human nAChRs subunits using structure-based design methods. It is highly desirable to find drugs that can selectively interact with different nAChR subtypes. In order to perform structure-based drug discovery for treatment of alcoholism, it is vital important to understand the 3D structures of nAChR $\alpha 3\beta 2$, $\alpha 3\beta 3$ and/or $\alpha 6$ subtypes, particularly their ligand-binding domain. However, so far no crystal structures for human nAChRs are available yet. Lack of information on the nAChR 3D structures has prevented attempts to design nAChR agonists with diverse specificity profiles.

nAChR is a well studied, pharmacologically important member of the Cys-loop superfamily of oentamiric ligand-gated ion channels (Albuquerque *et al.*, 2009). They are composed of five membrane-spanning sub-units arranged around a central pore (Wells, 2008). There are two groups of nAChRs: the muscle type and neuronal type, consisted of a variety of subunits in different combinations. A variety of nAChR subtypes are known to exist, depending on different subunit assemblies ($\alpha 1$ - $\alpha 10$, $\beta 1$ - $\beta 4$, δ , γ and ϵ) (Alkondon and Albuquerque, 2004). They are composed of a large N-terminal ECD (also called ligand-binding domain, LED), four hydrophobic transmembrane regions (M1-M4), one intracellular domain joining M3 and M4 and a small extracellular C-terminal domain.

The current interest in nAChRs stems from the fact they are important pharmaceutical targets for many human diseases, such as cognitive and attention deficits, Alzheimer's disease, Parkinson's disease, epilepsy, schizophrenia, anxiety, pain management, as well as for cessation of smoking and alcohol drinking (Steinlein and Bertrand, 2008). In order to treat these diseases, it would be helpful to design drugs that can selectively interact with different nAChR subtypes. For this purpose, it is important to have a detailed knowledge of nAChRs ligand binding site.

The first breakthrough in the investigation of the structure of ECD of nAChRs was the elucidation of the X-ray structure of a soluble acetylcholine-binding protein (AChBP) which is a functional homologue of the ECD of nAChRs (Brejci *et al.*, 2001). Since then, several crystal structures of AChBP have been reported, providing structural details of the interaction between the ECD and variety of agonists and antagonists (Celie *et al.*, 2004; Bourne *et al.*, 2005; Hansen *et al.*, 2005; Celie *et al.*, 2005; Unwin, 2005; Ihara *et al.*, 2008). AChBP has the same pentameric assembly as nAChRs and shares ~24% sequence identity with nAChRs. The discovery of AChBP has paved the way to the construction of structural models of the nAChR's LED using homology modeling (Krieger *et al.*, 2003) and has been extensively used as a model to investigate structural and dynamic features of nAChRs. Models of nAChR subtypes $\alpha 7$

(Schapira *et al.*, 2002; Le Novère *et al.*, 2002; Huang *et al.*, 2008; Mordvitsev *et al.*, 2007; Amiri *et al.*, 2005; Chou, 2004; Bisson *et al.*, 2008), $\alpha 4\beta 2$ (Schapira *et al.*, 2002; Le Novère *et al.*, 2002; Bisson *et al.*, 2008; Huang *et al.*, 2005; Haddadian *et al.*, 2008), $\alpha 4\beta 4$ (Schapira *et al.*, 2002), $\alpha 3\beta 4$ (Costa *et al.*, 2003), $\alpha 3\beta 2$ (Hu and Southerland, 2007; Schapira *et al.*, 2002), $\alpha 9\alpha 10$ (Pérez *et al.*, 2009), and $(\alpha 1)_2(\beta 1)\gamma\delta$ (Le Novère *et al.*, 2002; Mordvitsev *et al.*, 2007; Mordvitsev *et al.*, 2005) have been reported.

A further breakthrough in the structure studies of the nAChRs was the recent crystal structure determination of the entire N-terminal extracellular domain of the mouse nAChR $\alpha 1$ subunit bound to α -bungarotoxin at 1.94 Å resolution (Dellisanti *et al.*, 2007). Since this structure provides the first high-resolution view of the ECD of nAChRs and is better than AChBP to be used to model the ECD of the human nAChR subunits due to the high degree of homology between them, it is a good template for the modeling of the ECD of the human nAChRs. Model of the ECD of the human $\alpha 7$ nAChR based on the 3D structure of the mouse $\alpha 1$ nAChR ECD has been reported (Konstantakaki *et al.*, 2008).

Using the crystal structure of the mouse $\alpha 1$ nAChR ECD as a template, we have built both monomer and pentamer models of the LED of human nAChR $\alpha 3\beta 2$, $\alpha 4\beta 2$, $\alpha 3\beta 3$, $\alpha 6$, and $\alpha 7$ subunits by computational homology modeling. The resulting models provide molecular targets for structure-based design of subtype-specific nAChR agonists. Computational docking study also was carried out to gain understanding on the interactions between nicotine and nAChR.

2 Methods

2.1 Preparation of the Sequence and Template

The amino acid sequences of the human nAChR $\alpha 3$ (hA3), $\alpha 4$ (hA4), $\alpha 6$ (hA6), $\alpha 7$ (hA7), $\beta 2$ (hB2), and $\beta 3$ (hB3) were obtained from the National Center for Biotechnology Institute (NCBI). The Uniprot accession number for hA3, hA4, hA6, hA7, hB2, and hB3, are P32297, P43681, Q15825, P36544, P17787, and Q05901, respectively. The sequences were first edited to remove the signal peptide segments. All subsequent amino acid numbering is based on the mature sequences without the signal peptide. The sequences were then edited to remove all of the residues beyond LED. The X-ray structure of the ECD of the $\alpha 1$ subunit of the mouse nAChR (Dellisanti *et al.*, 2007), the first X-ray structure obtained of a region of the nAChR (PDB: 2QC1), was used as the template and was edited so that it contained only the chain B, and hereafter it was referred to as 2QC1B.

2.2 Sequence Alignments

The edited sequences of six human nAChR monomers (hA3, hA4, hA6, hA7, hB2, and hB3) were first aligned to the ECD of the mouse nAChR $\alpha 1$ subunit template respectively using the BLAST server at NCBI (<http://blast.ncbi.nlm.nih.gov/>). They were further refined by aligning these six sequences with the structure of 2QC1B based on a dynamic programming algorithm present within the MODELLER software package (Sali and Blundell, 1993), which is different from standard sequence-sequence alignment methods because it takes into account structural information from the template when constructing an alignment. This task is achieved through a variable gap penalty function that tends to place gaps outside secondary structure segments (Fig. 1). This improvement becomes more important as the similarity between the sequences decreases and the number of gaps increases.

2.3 Homology Modeling

Based on the sequence alignment with the ECD of the $\alpha 1$ mouse subunit, the three-dimensional model of the LBD of six human nAChR monomers were built using the program MODELLER

(Sali and Blundell, 1993). The MODELLER's automodel command was invoked by a script (model-single.py) to automatically assign atomic coordinates to regions structurally aligned with the template, build intervening loops, optimize the rotamers of amino acid side chains, and perform an initial energy optimization of the structure, using the 2QC1B template structure and the alignment obtained in the previous sequence alignment stage (file: model-tem.ali). For each monomer, 5 models were generated, and the model with the lowest value of the MODELLER objective function was selected for further refinement.

The pentameric structures of the ECD of five human nAChR subunits, $\alpha 3\beta 2$, $\alpha 4\beta 2$, $\alpha 3\beta 3$, $\alpha 6$, and $\alpha 7$, were modeled using the X-ray structure of the AChBP pentamer (PDB: 1I9B) (Brejc *et al.*, 2001) as the template. The 3D structures were derived using Chimera program (Meng *et al.*, 2006) to superimpose corresponding human nAChR monomers to the A-, B-, C-, D, and E-chains of 1I9B consecutively.

The models generated were subjected to an overall energy minimization with respect to all atoms to finalize the entire pentamer structure using CHARMM program (Miller *et al.*, 2008; Kim *et al.*, 2008; Brooks *et al.*, 1983). The energy calculation and minimization was performed with GBMV (Generalized Born using Molecular Volume) implicit solvation model. This model mimics the Poisson-Boltzmann (PB) electrostatic solvation energy calculation using a generalized Born method, which allows the computation of solvation energies very similar to the PB equations. The PB method has been considered a benchmark for implicit solvation calculations (Lee *et al.*, 2003). The resulting models were used for next molecular docking and virtual screening step without any further refinement.

2.4 Docking of nicotine with the homodimer

The docking of nicotine was performed with the program WinDock developed in our laboratory (Hu and Southerland, 2007), which uses the widely distributed DOCK searching engine (Ewing *et al.*, 2001; Moustakas *et al.*, 2006) to dock flexible small molecules to macromolecular sites, and to evaluate the binding affinity of ligands. WinDock's SPHBOC module was used to determine the binding site and produce a set of spheres for binding site characterization. Contact scores and energy scores were calculated using an energy cutoff distance of 6.0 Å and a van der Waals repulsive exponent of 8.0 Å. Ligands were oriented to the spheres with a distance tolerance of 0.5 Å and distance minimum of 2.0 Å. A minimum anchor size of 50 was used with an internal energy repulsive exponent of 8.0 Å and clash overlap of 0.25 Å. All other parameters were left as their defaults.

3 Results

3.1 Sequence Alignments

Since the structure of a protein is uniquely determined by its sequence and similar sequence fold into similar structures, it is possible to obtain the structure of a protein by sequence alignment of its sequence with knowing protein structure (Krieger *et al.*, 2003; Rost, 1999), as long as the length of two sequences and the percentage of identical residues fall in the region marked as "safe" in Fig. 2. Protein sequence alignments thus unambiguously distinguish between protein pairs of similar and non-similar structure (Rost, 1999). Based on the sequence alignment, the structure of the ECD of the mouse nAChR $\alpha 1$ subunit is better than AChBP to be used to model the ECD of the human nAChR subunits due to the high degree of homology between them (Table 1 and Fig. 2), which is about 50% higher than the degree of identity between the ECDs of the human nAChR subunits and AChBP.

3.2 Human nAChR monomers

The overall 3D structural model of the ECD for human nAChR monomers were given in Fig. 3. As expected from the low number of insertions/deletions, the model of the ECD of the human nAChR monomers does not differ largely from that of the template. It consists of an N-terminal α -helix followed by ten strands that form a β -sandwich. The inner sheet is made of strands β 1, β 2, β 3, β 6, and β 8, whereas the outer sheet is made of strands β 4, β 7, β 9, and β 10. A disulphide bond is formed between Cys128 on the inner sheet and Cys142 on the outer sheet, linking the two sheets together. Investigation has shown that loops β 4- β 5 (A), β 7- β 8 (B), and β 9- β 10 (C) serves as the principle ligand-binding elements (Brejc *et al.*, 2001; Sin and Engel, 2006; Unwin, 2005), while loops β 1- β 2, β 6- β 7 (Cys loop), and β 8- β 9, three membrane-facing loops, has the important role in the interaction between the ECD and the transmembrane domain during ligand-induced gating (Dellisanti *et al.*, 2007).

The 13-residue Cys loop, which is highly conserved in the nAChRs, adopts a similar structure to that of the mouse α 1 ECD as a type VIb turns. Phe135, located the tip of the Cys-loop, has the structural role to maintain this unique conformation and has been shown to be a key residue for the function of nAChR (Dellisanti *et al.*, 2007).

3.3 Human nAChR pentamers

Like the AChBP pentamer, the resulting 3D structural model of the ECD of human nAChR shows fivefold symmetry when viewed along the axis (Fig. 4). It was a barrel of 80 Å diameter and 63 Å height with a central irregular pore (10–15 Å).

The comparison of the structure of the mouse α 1 ECD with that of AChBP and the electron microscopic model of the *Torpedo* nAChR pentamer indicated that monomeric state of the mouse α 1 ECD crystal structure does not significantly affects its structure, especially in regions that are expected to interact with the adjacent subunits (Dellisanti *et al.*, 2007). Therefore, the modeled structures of the ECD of human nAChR pentamer could be used to investigate the ligand binding.

3.4 The ligand binding site

The model of the ligand-binding pocket of the human α 3 β 2 nAChR dimer and its complex with nicotine is shown in Fig. 5. The dimer interface is formed by an interlocking array of neighboring chain secondary structure elements. The residues involved in the dimer interface are listed in Table 2. The interface consists of 18 residues (16 for α 6 dimer), of which 8 or 7 are from chain A and rest from chain B.

The ligand-binding pockets of the human nAChRs are formed by loops A, B, and C of the principal component (chain A) and loops D and E of the complementary component (chain B) of the adjacent subunit. The key residues of the loops involved in the formation of the ligand-binding site are Tyr93 from loop A, Ser 148 and Trp149 from loop B, and Tyr190 and Tyr195 from loop C (all these residues belong to chain A and use mouse α 1 numbering), and Trp57 from loop D (residues from chain B).

Identification of all residues involved in the ligand binding (e.g. agonists, competitive antagonists, and noncompetitive agonists) is a primary objective to understand which structural components are related to the physiological function of nAChR. The position of the ligand in the current models is in good agreement with the results of biochemical experiments performed on *Torpedo* nAChR. According to the mutagenesis experiments, residue Trp149 is able to establish a π -cation interaction with the ammonium group of acetylcholine (Zhong *et al.*, 1998). Moreover, photolabeling experiments have shown that residues Tyr190 and Tyr198 in α subunit were the principal amino acids labeled by [3H]nicotine (Middleton and Cohen,

1991), residue Trp55 was the primary site of [3H]nicotine photoincorporation within a non- α -subunit (Chiara *et al.*, 1998), and residues Tyr190 and Tye198 involved primarily in the interaction with the ester moiety of acetylcholine (Grutter *et al.*, 2000). In addition, residue Tyr93 within α subunit was identified as contributing to the cation-binding domain of the AChR agonist-binding site (Cohen *et al.*, 1991). All these residues mentioned are key residues in the ligand-binding pockets of our ECD models of the human nAChR $\alpha 3\beta 2$, $\alpha 3\beta 3$, $\alpha 4\beta 2$, $\alpha 6$, and $\alpha 7$ subunits (Table 2). Furthermore, the ligand-binding site of our human nAChR $\alpha 7$ model is formed essentially by the same residues as those in the chicken $\alpha 7$ nAChR modeled previously (Le Novère *et al.*, 2002). The key residues involved in the formation of the ACh-binding site are also involved in the formation of nicotine-binding site: Tyr93, Trp149, Tyr151, Tyr188, Cys190 and Tyr195 from chain A, and Trp55, Leu109, Gln117, and Leu119 from chain B.

Investigations have indicated that the major role of α subunits of nAChRs in the channel gating process is proving the principle binding surface (the plus side) (Brejc *et al.*, 2001; Sin and Engel, 2006; Unwin, 2005). It could be shown (Fig. 1 and Table 2) that residues from the principle subunit involved in ligand binding are generally conserved (the residues in bold in Table 2), whereas the residues in the complementary part (minus side) of the binding site shown more variation. Previous studies have indicated that the β subunits confer agonist selectivity to the nAChRs (Cohen *et al.*, 1995; Luetje and Patrick, 1991; Parker *et al.*, 1998; 2001), it is therefore possible to design nAChR subtype-specific drugs according to the difference between ligand binding sites of human nAChRs.

4 Conclusion

Alcoholism and alcohol abuse are one of the most prevalent neuropsychiatric diseases and have an enormous health and socioeconomic impact. The human nAChR $\alpha 3\beta 2$, $\alpha 3\beta 3$, and $\alpha 6$ subtypes have been shown to be neurochemical targets for developing new drugs in the treatment of alcoholism. To discover new drugs using structure-based method, it is important to find the 3D structures of these human nAChR subtypes. Based on the crystal structure of the ECD of the mouse $\alpha 1$ nAChR, the ECD models of the human nAChR $\alpha 3\beta 2$, $\alpha 3\beta 3$, $\alpha 4\beta 2$, $\alpha 6$, and $\alpha 7$ subunits was constructed using comparative modeling. The 3D models of the ECD of the monomer, and pentamer of these human nAChRs were constructed. The docking of the agonist nicotine in the ligand-binding pocket of the human nAChR dimers was also performed. Since the nAChR ligand-binding site is a useful target for mutagenesis studies and the rational design of drugs that can selectively activate different human nAChR subtypes against various diseases, these models provide structural frames for future investigation.

Acknowledgments

This work is supported by grant RCMI-NIH 2G12RR03048.

References

1. Albuquerque EX, Pereira EF, Alkondon M, Rogers SW. Mammalian nicotinic acetylcholine receptors: from structure to function. *Physiol Rev* 2009;89:73–120. [PubMed: 19126755]
2. Alkondon M, Albuquerque EX. The nicotinic acetylcholine receptor subtypes and their function in the hippocampus and cerebral cortex. *Prog Brain Res* 2004;145:109–120. [PubMed: 14650910]
3. Amiri S, Tai K, Beckstein O, Biggin PC, Sansom MS. The $\alpha 7$ nicotinic acetylcholine receptor: molecular modelling, electrostatics, and energetics. *Mol Membr Biol* 2005;22:151–162. [PubMed: 16096259]
4. Bisson WH, Westera G, Schubiger PA, Scapozza L. Homology modeling and dynamics of the extracellular domain of rat and human neuronal nicotinic acetylcholine receptor subtypes $\alpha 4\beta 2$ and $\alpha 7$. *J Mol Model* 2008;14:891–899. [PubMed: 18607650]

5. Bourne Y, Talley TT, Hansen SB, Taylor P, Marchot P. Crystal structure of a CbtX-AChBP complex reveals essential interactions between snake alpha-neurotoxins and nicotinic receptors. *EMBO J* 2005;24:1512–1522. [PubMed: 15791209]
6. Brejc K, van Dijk WJ, Klaassen RV, Schuurmans M, van Der Oost J, Smit AB, Sixma TK. Crystal structure of an ACh-binding protein reveals the ligand-binding domain of nicotinic receptors. *Nature* 2001;411:269–276. [PubMed: 11357122]
7. Brooks BR, Bruccoleri RE, Olafson BD, States DJ, Swaminathan S, Karplus M. CHARMM: A program for macromolecular energy, minimization, and dynamics calculations. *J Comp Chem* 1983;4:187–217.
8. Celie PH, Kasheverov IE, Mordvintsev DY, Hogg RC, van Nierop P, van Elk R, van Rossum-Fikkert SE, Zhmak MN, Bertrand D, Tsetlin V, Sixma TK, Smit AB. Crystal structure of nicotinic acetylcholine receptor homolog AChBP in complex with an alpha-conotoxin PnIA variant. *Nat Struct Mol Biol* 2005;12:582–588. [PubMed: 15951818]
9. Celie PH, van Rossum-Fikkert SE, van Dijk WJ, Brejc K, Smit AB, Sixma TK. Nicotine and carbamylcholine binding to nicotinic acetylcholine receptors as studied in AChBP crystal structures. *Neuron* 2004;41:907–914. [PubMed: 15046723]
10. Chiara DC, Middleton RE, Cohen JB. Identification of tryptophan 55 as the primary site of [3H] nicotine photoincorporation in the gamma-subunit of the Torpedo nicotinic acetylcholine receptor. *FEBS Lett* 1998;423:223–226. [PubMed: 9512361]
11. Chou KC. Insights from modelling the 3D structure of the extracellular domain of $\alpha 7$ nicotinic acetylcholine receptor. *Biochem Biophys Res Commun* 2004;319:433–438. [PubMed: 15178425]
12. Cohen BN, Figl A, Quick MW, Labarca C, Davidson N, Lester HA. Regions of beta 2 and beta 4 responsible for differences between the steady state dose-response relationships of the alpha 3 beta 2 and alpha 3 beta 4 neuronal nicotinic receptors. *J Gen Physiol* 1995;105:745–764. [PubMed: 7561742]
13. Cohen JB, Sharp SD, Liu WS. Structure of the agonist-binding site of the nicotinic acetylcholine receptor. [3H] acetylcholine mustard identifies residues in the cation-binding subsite. *J Biol Chem* 1991;266:23354–23364. [PubMed: 1744130]
14. Costa V, Nistri A, Cavalli A, Carloni P. A structural model of agonist binding to the alpha3beta4 neuronal nicotinic receptor. *Br J Pharmacol* 2003;140:921–931. [PubMed: 14504134]
15. Dellisanti CD, Yao Y, Stroud JC, Wang ZZ, Chen L. Crystal structure of the extracellular domain of nAChR alpha1 bound to alpha-bungarotoxin at 1.94 Å resolution. *Nat Neurosci* 2007;10:953–962. [PubMed: 17643119]
16. Ewing TJ, Makino S, Skillman AG, Kuntz ID. DOCK 4.0: search strategies for automated molecular docking of flexible molecule databases. *J Comput Aided Mol Des* 2001;15:411–428. [PubMed: 11394736]
17. Gao GY, Li DJ, Keung WM. Synthesis of daidzin analogues as potential agents for alcohol abuse. *Bioorg Med Chem* 2003;11:4069–4081. [PubMed: 12927869]
18. Grutter T, Ehret-Sabatier L, Kotzyba-Hibert F, Goeldner M. Photoaffinity labeling of Torpedo nicotinic receptor with the agonist [3H]DCTA: identification of amino acid residues which contribute to the binding of the ester moiety of acetylcholine. *Biochemistry* 2000;39:3034–3043. [PubMed: 10715124]
19. Haddadian EJ, Cheng MH, Coalson RD, Xu Y, Tang P. In silico models for the human alpha4beta2 nicotinic acetylcholine receptor. *J Phys Chem B* 2008;112:13981–13990. [PubMed: 18847252]
20. Hansen SB, Sulzenbacher G, Huxford T, Marchot P, Taylor P, Bourne Y. Structures of Aplysia AChBP complexes with nicotinic agonists and antagonists reveal distinctive binding interfaces and conformations. *EMBO J* 2005;24:3635–3646. [PubMed: 16193063]
21. Hu Z, Southerland W. WinDock: structure-based drug discovery on Windows-based PCs. *J Comput Chem* 2007;28:2347–2351. [PubMed: 17476686]
22. Huang X, Zheng F, Crooks PA, Dwoskin LP, Zhan CG. Modeling multiple species of nicotine and deschloroepibatidine interacting with alpha4beta2 nicotinic acetylcholine receptor: from microscopic binding to phenomenological binding affinity. *J Am Chem Soc* 2005;127:14401–14414. [PubMed: 16218635]

23. Huang X, Zheng F, Stokes C, Papke RL, Zhan CG. Modeling binding modes of alpha7 nicotinic acetylcholine receptor with ligands: the roles of Gln117 and other residues of the receptor in agonist binding. *J Med Chem* 2008;51:6293–6302. [PubMed: 18826295]
24. Ihara M, Okajima T, Yamashita A, Oda T, Hirata K, Nishiwaki H, Morimoto T, Akamatsu M, Ashikawa Y, Kuroda S, Mega R, Kuramitsu S, Sattelle DB, Matsuda K. Crystal structures of *Lymnaea stagnalis* AChBP in complex with neonicotinoid insecticides imidacloprid and clothianidin. *Invert Neurosci* 2008;8:71–81. [PubMed: 18338186]
25. Jerlhag E, Eggecioglu E, Dickson SL, Svensson L, Engel JA. Alpha-conotoxin MII-sensitive nicotinic acetylcholine receptors are involved in mediating the ghrelin-induced locomotor stimulation and dopamine overflow in nucleus accumbens. *Eur Neuropsychopharmacol* 2008;18:508–518. [PubMed: 18343642]
26. Jerlhag E, Grøtli M, Luthman K, Svensson L, Engel JA. Role of the subunit composition of central nicotinic acetylcholine receptors for the stimulatory and dopamine-enhancing effects of ethanol. *Alcohol* 2006;41:486–493.
27. Jo S, Kim T, Iyer VG, Im W. CHARMM-GUI: a web-based graphical user interface for CHARMM. *J Comput Chem* 2008;29:1859–1865. [PubMed: 18351591]
28. Konstantakaki M, Tzartos SJ, Poulas K, Eliopoulos E. Model of the extracellular domain of the human alpha7 nAChR based on the crystal structure of the mouse alpha1 nAChR extracellular domain. *J Mol Graph Model* 2008;26:1333–1337. [PubMed: 18329305]
29. Krieger, E.; Nabuurs, SB.; Vriend, G. Homology modeling. In: Bourne, PE.; Weissig, H., editors. *Structural bioinformatics*. New Jersey: Wiley-Liss, Hoboken; 2003. p. 509-524.
30. Larsson A, Engel JA. Neurochemical and behavioral studies on ethanol and nicotine interactions. *Neurosci Biobehav Rev* 2004;27:713–720. [PubMed: 15019421]
31. Le Novère N, Grutter T, Changeux JP. Models of the extracellular domain of the nicotinic receptors and of agonist- and Ca²⁺ binding sites. *Proc Natl Acad Sci USA* 2002;99:3210–3215. [PubMed: 11867716]
32. Lee MS, Feig M, Salsbury FR Jr, Brooks CL 3rd. New analytic approximation to the standard molecular volume definition and its application to generalized Born calculations. *J Comput Chem* 2003;24:1348–1356. [PubMed: 12827676]
33. Luetje CW, Patrick J. Both alpha- and beta-subunits contribute to the agonist sensitivity of neuronal nicotinic acetylcholine receptors. *J Neurosci* 1991;11:837–845. [PubMed: 1705971]
34. Meng EC, Pettersen EF, Couch GS, Huang CC, Ferrin TE. Tools for integrated sequence-structure analysis with UCSF Chimera. *BMC Bioinformatics* 2006;7:339–349. [PubMed: 16836757]
35. Middleton RE, Cohen JB. Mapping of the acetylcholine binding site of the nicotinic acetylcholine receptor: [3H]nicotine as an agonist photoaffinity label. *Biochemistry* 1991;30:6987–6997. [PubMed: 2069955]
36. Miller BT, Singh RP, Klauda JB, Hodosek M, Brooks BR, Woodcock HL 3rd. CHARMMing: a new, flexible web portal for CHARMM. *J Chem Inf Model* 2008;48:1920–1929. [PubMed: 18698840]
37. Mordvintsev DY, Polyak YL, Levtsova OV, Tourleigh YV, Kasheverov IE, Shaitan KV, Utkin YN, Tsetlin VI. A model for short alpha-neurotoxin bound to nicotinic acetylcholine receptor from *Torpedo californica*: Comparison with long-chain alpha-neurotoxins and alpha-conotoxins. *Comput Biol Chem* 2005;29:398–411. [PubMed: 16290328]
38. Mordvitsev DY, Polyak YL, Kuzmin DA, Levtsova OV, Tourleigh YV, Utkin YN, Shaitan KV, Tsetlin VI. Computer modeling of binding of diverse weak toxins to nicotinic acetylcholine receptors. *Comput Biol Chem* 2007;31:72–81. [PubMed: 17392029]
39. Moustakas DT, Lang PT, Pegg S, Pettersen E, Kuntz ID, Brooijmans N, Rizzo RC. Development and validation of a modular, extensible docking program: DOCK 5. *J Comput Aided Mol Des* 2006;20:601–619. [PubMed: 17149653]
40. Narahashi T, Aistrup GL, Marszalec W, Nagata K. Neuronal nicotinic acetylcholine receptors: a new target site of ethanol. *Neurochem Int* 1999;35:131–141. [PubMed: 10405997]
41. Parker MJ, Beck A, Luetje CW. Neuronal nicotinic receptor beta2 and beta4 subunits confer large differences in agonist binding affinity. *Mol Pharmacol* 1998;54:1132–1139. [PubMed: 9855644]

42. Parker MJ, Harvey SC, Luetje CW. Determinants of agonist binding affinity on neuronal nicotinic receptor beta subunits. *J Pharmacol Exp Ther* 2001;299:385–391. [PubMed: 11561103]
43. Pérez EG, Cassels BK, Zapata-Torres G. Molecular modeling of the alpha9alpha10 nicotinic acetylcholine receptor subtype. *Bioorg Med Chem Lett* 2009;19:251–254. [PubMed: 19013796]
44. Rost B. Twilight zone of protein sequence alignments. *Protein Eng* 1999;12:85–94. [PubMed: 10195279]
45. Sali A, Blundell TL. Comparative protein modelling by satisfaction of spatial restraints. *J Mol Biol* 1993;234:779–815. [PubMed: 8254673]
46. Schapira M, Abagyan R, Totrov M. Structural model of nicotinic acetylcholine receptor isotypes bound to acetylcholine and nicotine. *BMC Struct Biol* 2002;2:1–8. [PubMed: 11860617]
47. Sine SM, Engel AG. Recent advances in Cys-loop receptor structure and function. *Nature* 2006;440:448–455. [PubMed: 16554804]
48. Spanagel R, Kiefer F. Drugs for relapse prevention of alcoholism: ten years of progress. *Trends Pharmacol Sci* 2008;29:109–115. [PubMed: 18262663]
49. Steinlein OK, Bertrand D. Neuronal nicotinic acetylcholine receptors: from the genetic analysis to neurological diseases. *Biochem Pharmacol* 2008;76:1175–1183. [PubMed: 18691557]
50. Unwin N. Refined structure of the nicotinic acetylcholine receptor at 4Å resolution. *J Mol Biol* 2005;346:967–989. [PubMed: 15701510]
51. Wells GB. Structural answers and persistent questions about how nicotinic receptors work. *Front Biosci* 2008;13:5479–5510. [PubMed: 18508600]
52. Zhong W, Gallivan JP, Zhang Y, Li L, Lester HA, Dougherty DA. From ab initio quantum mechanics to molecular neurobiology: a cation-pi binding site in the nicotinic receptor. *Proc Natl Acad Sci USA* 1998;95:12088–12093. [PubMed: 9770444]

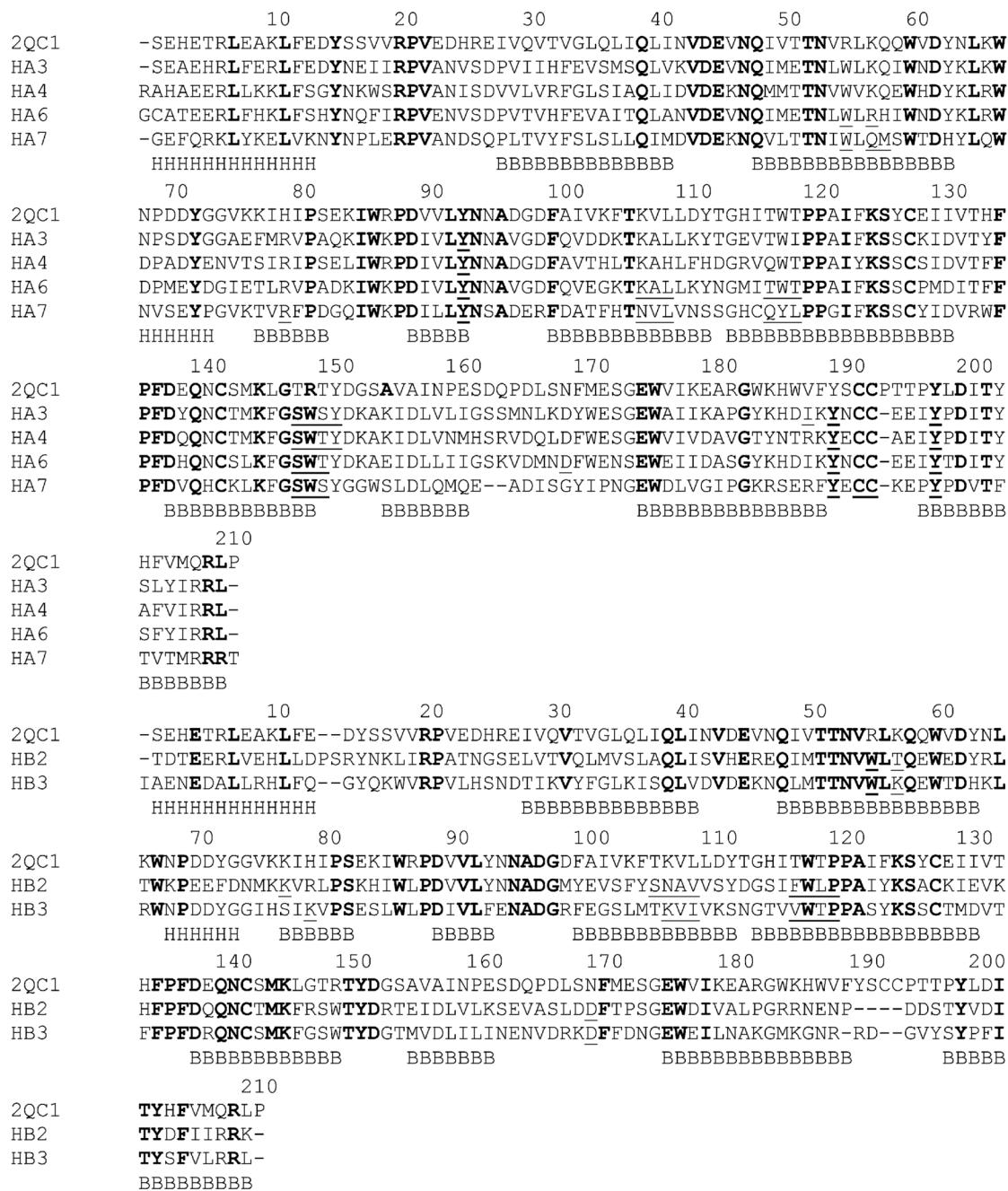


Fig. 1. Multiple sequence alignment of the ECDs of the mouse $\alpha 1$ with human nAChR monomers. The alignment was divided into subunit 1 monomers (top, $\alpha 3$, $\alpha 4$, $\alpha 6$, and $\alpha 7$) and subunit 2 monomers (bottom, $\beta 2$, and $\beta 3$). Identical residues are shown in bold, while residues involved in ligand binding are shown in underline. Secondary structure elements are shown under the sequences: H= a-helix, B=b-strand.

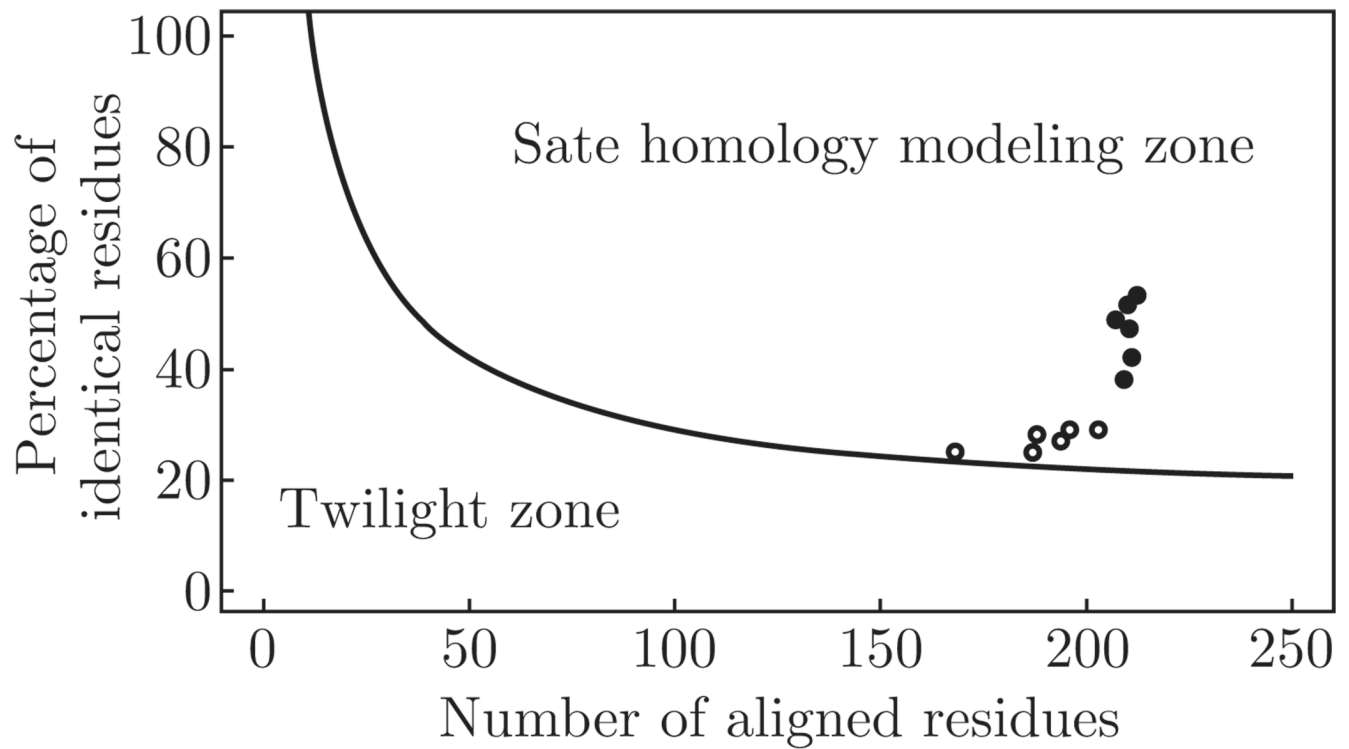


Fig. 2.

The two zones of protein sequence alignments. Two sequences are practically guaranteed to adopt a similar structure if their length and percentage sequence identity fall into the region marked as “safe”. A heavy black dot represents the degree of homology between the ECDs of the mouse $\alpha 1$ and human nAChR monomers; a circle represents the degree of homology between the ECDs of AChBP and human nAChR monomers.

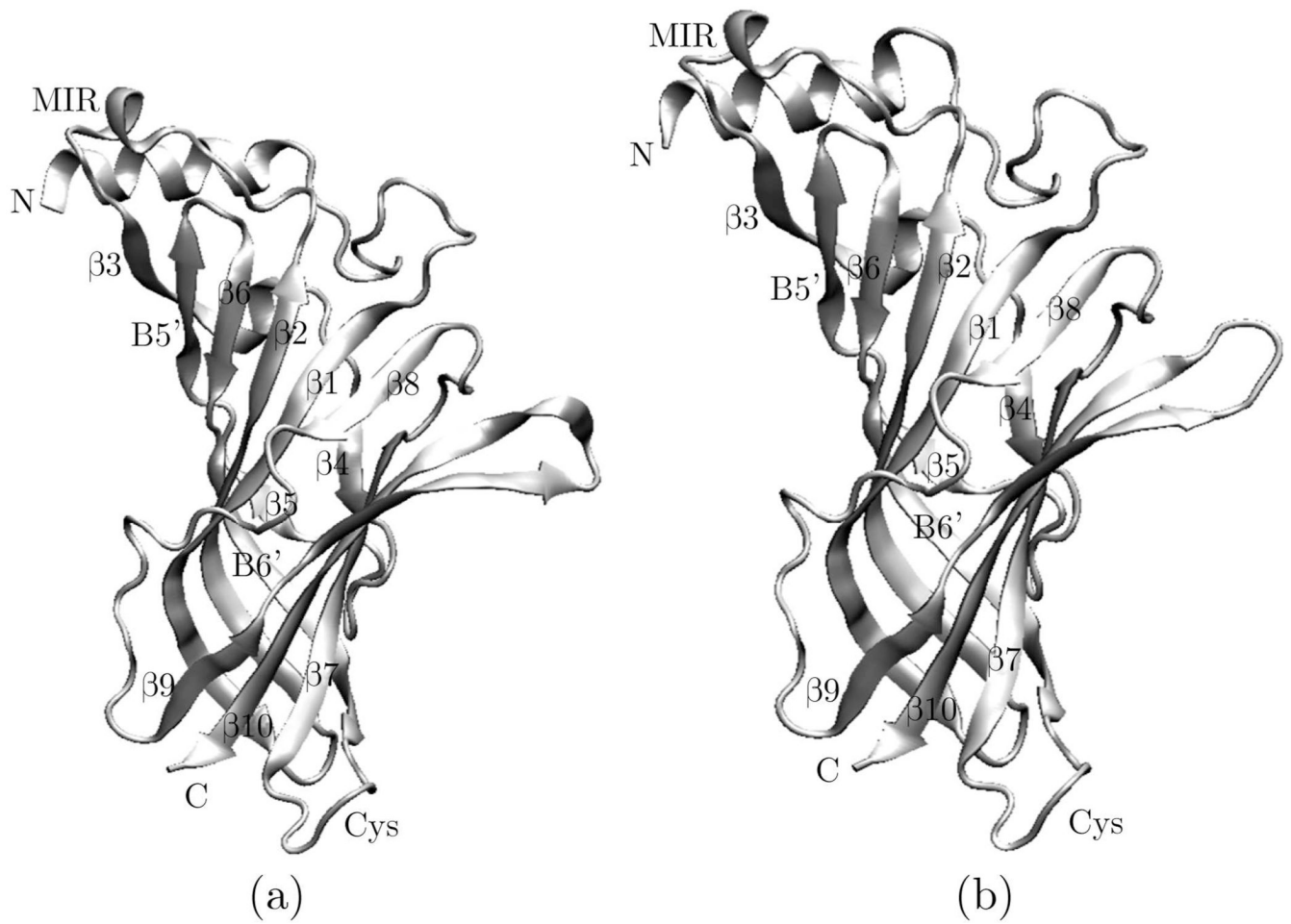


Fig. 3. Model of the ECD of the human nAChR monomer based on the sequence alignment shown in Fig. 1 and subsequent homology modeling. (a) $\alpha 3$ monomer, (b) $\beta 2$ monomer.

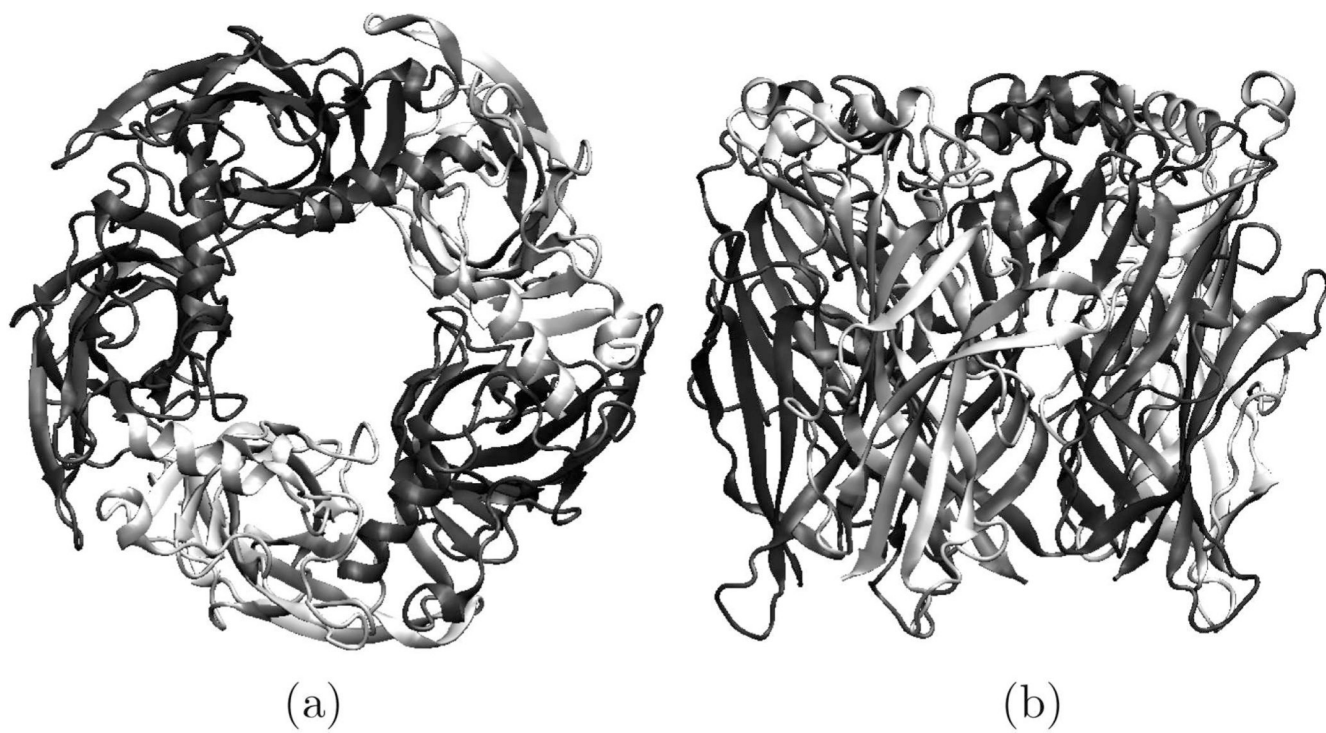


Fig. 4. Model of the ECD of the human nAChR pentamer. (a) side view and (b) top view.

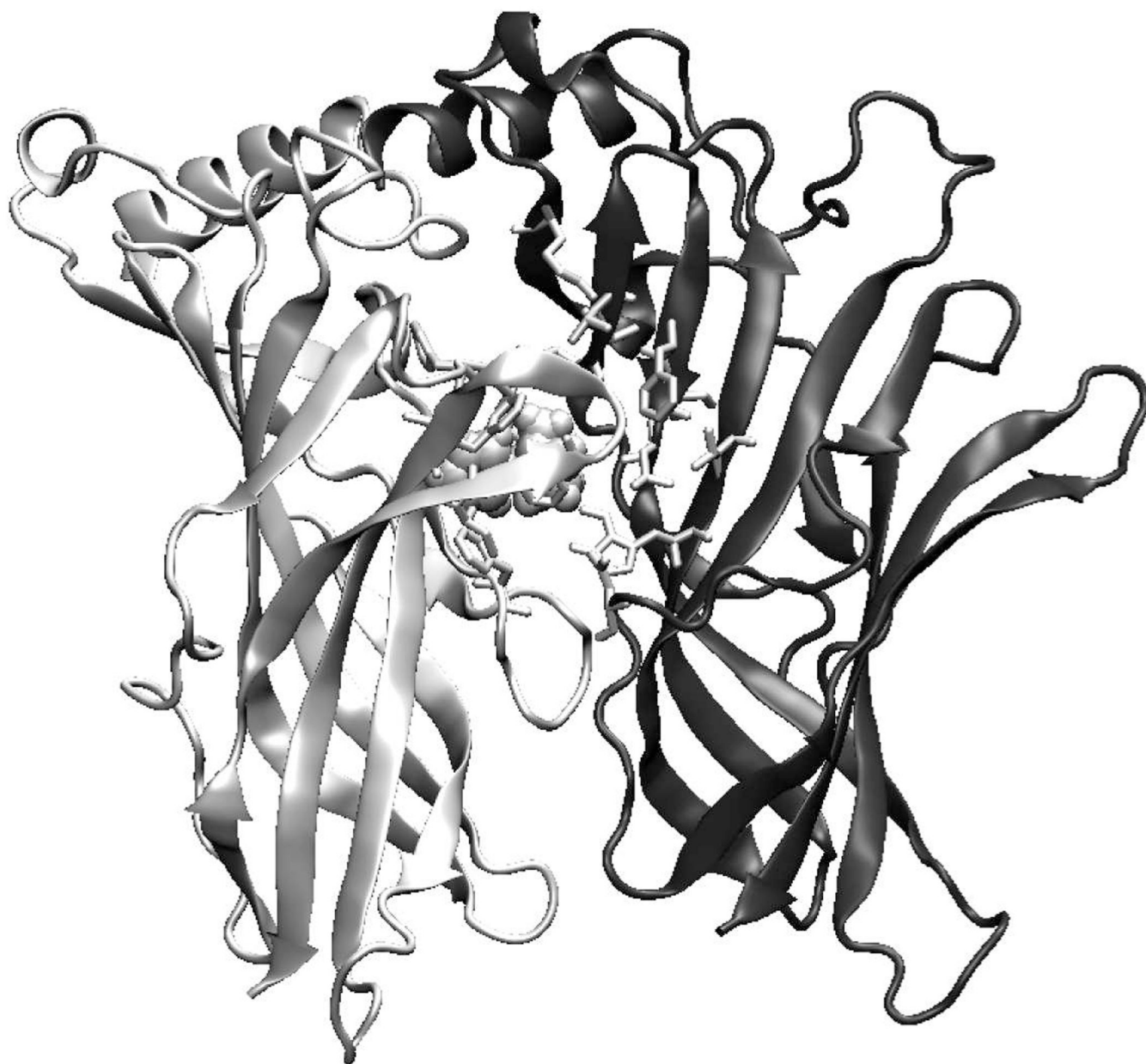


Fig. 5. Ligand-binding site of the human $\alpha 3\beta 2$ nAChR dimer model with nicotine bound (shown in sphere). The principal component ($\alpha 3$) is shown in light grey and the complementary component ($\beta 2$) in dark grey. All key residues discussed in the text are shown in stick.

Table 1

The degree of residue identity between the ECDs of the mouse $\alpha 1$ nAChR subunit and the human nAChR monomers (identity of residues with AchBP is included for comparison)

TYPE	2QC1B		2BR7	
	Identities	Gaps	Identities	Gaps
$\alpha 3$	108/210 (51%)	1/210 (0%)	54/188 (28%)	4/188 (2%)
$\alpha 4$	110/211 (52%)	1/211 (0%)	59/203 (29%)	6/203 (2%)
$\alpha 6$	102/207 (49%)	1/207 (0%)	57/196 (29%)	6/196 (3%)
$\alpha 7$	80/209 (38%)	3/209 (1%)	54/194 (27%)	14/194 (7%)
$\beta 2$	89/211 (42%)	6/211 (2%)	42/168 (25%)	8/168 (4%)
$\beta 3$	99/210 (47%)	3/210 (1%)	47/187 (25%)	6/187 (3%)

Table 2

Residues involved in the ligand binding at human nAChR dimer interface

Chain	$\alpha 3\beta 2$	$\alpha 3\beta 3$	$\alpha 4\beta 2$	$\alpha 6\alpha 6$	$\alpha 7\alpha 7$
A	TYR93	TYR93	TYR98	TYR98	TYR93
	SER148	SER148	SER153	SER153	SER148
	TRP149	TRP149	TRP154	TRP154	TRP149
	SER150	SER150	THR155	THR155	SER150
	TYR151		TYR156		
	ILE188	ILE188		ILE193	
	TYR190	TYR190	TYR195	TYR195	TYR188
					CYS190
					CYS191
		TYR197	TYR197	TYR202	TYR202
B	TRP57	TRP56	TRP57	TRP60	TRP55
	THR59	LYS58	THR59	ARG62	GLN57
					MET58
	LYS79				
		LYS80			
			SER108		ARG79
	ASN109	LYS108	ASN109	LYS112	ASN107
	ALA110	VAL109	ALA110	ALA113	VAL108
	VAL111	ILE110	VAL111	LEU114	LEU109
	PHE119	VAL118	PEH119	THR122	GLN117
TRP120	TRP119	TRP120	TRP123	TYR118	
LEU121	THR120	LEU121	THR124	LEU119	
	PRO121	PRO122			
ASP171	ASP170	ASP171	ASP174		